Plastic Deformation Capacity of Welded Beam-end Limited by Brittle Fracture

by

Takahiko Suzuki[1], Takumi Ishii[2], Yoshifumi Sakumoto[3] and Akiyoshi Mukai[4]

ABSTRACT

This paper proposes a method of assessing the plastic deformation capacity of welded beam-ends limited by brittle fracture. The phenomenon of brittle fractures in welded beam-ends was first observed in the 1995 Hyogo-ken Nanbu Earthquake, because a practical design method for preventing such fractures had yet to be established. It was, however, confirmed that the fracture toughness of the beam-end welds is one of the many factors controlling the initiation of fracture through full-scale tests conducted after the earthquake. This paper presents a relationship between fracture toughness and fracture strength of beam-end welded joints, which is obtained from the test results, and indicates that the plastic deformation capacity of beams can be calculated from the fracture strength. Further, a simple design expression for calculating the plastic rotation of the beams up to the fracture is presented using the representative stress-strain relation models of steel for buildings. The application of these approaches will allow structural designers to prevent beam-end brittle fractures, even during severe earthquakes, through the selection of suitable steels.

KEYWORDS: Brittle Fracture, Fracture Toughness, Plastic Deformation Capacity, Welded Beam-to-Column Connections

1. INTRODUCTION

In the Hyogo-ken Nanbu Earthquake, there was only limited damage of the collapse of steel buildings. Many fractures, however, were observed, mainly in the welded beam-to-column connections of square tube columns and H-shape beams. These fractures, which occured with buckling and plastification of the beams, were different from the fracture observed in the Northridge Earthquake. Further, it was confirmed that the fractures initiated from the end of beam-flange welded joint or the toe of weld access hole.

In the "strong column-weak beam" seismic design, the beam-end plastic deformation capacity is expected. Further, the deformation capacity was thought to be limited by local buckling, and then the method of calculating the deformation capacity, which is currently used in practical design, was proposed [1]. However, the damage in the Hyogo-ken Nanbu Earthquake presented that the deformation capacity is occasionally governed by fracture, and therefore a new method is needed.

It is possible to predict beam's deformation behaviors from the sectional shape and dimension of the beams and from stress-strain relations. In addition, it can be thought that the beam-end plastic deformation capacity is decided by ending the beam's deformation behavior due to the brittle fracture of beam-end flange. That is, if the fracture strength of beam-flange welded joint is known, the deformation capacity can be assessed by calculating the plastic deformation at the point where the tension force acting on the beam flange reaches its fracture strength.

Prior to the Hyogo-ken Nanbu Earthquake, the importance of fracture toughness, which is evaluated by the Charpy V-notch impact absorbed energy in this paper, was recognized, but experimental data concerning the influence of fracture toughness on the brittle fracture at beam-end were not

[1] Senior Researcher, Steel Structure Development Center, Nippon Steel Corporation, Futtsu-shi, Chiba-ken, 293-8511 Japan

[2] Senior Researcher, Civil Engineering Department, JFE R&D Corporation, Kawasaki-shi, Kanagawa-ken, 210-0855 Japan

[3] General Manager, Building Products Construction Materials Development Division, Nippon Steel Corporation, Chiyoda-ku, Tokyo, 100-8071 Japan

[4] Senior Research Engineer, Structural Engineering Department, Building Research Institute, Tsukuba-shi, Ibaraki-ken, 305-0802 Japan

available. After the Hyogo-ken Nanbu Earthquake, the conditions leading to the fracture were investigated through many full-scale tests and the importance of fracture toughness has become clear.

In this paper, the relationship between fracture strength and fracture toughness of the beam-flange welded joints is quantitatively determined based on data from existing full-scale tests. Next, a method is presented to assess beam-end plastic deformation capacity based on the fracture strength. In addition, a simple design expression for calculating the maximum plastic rotation of beams, which is decided by beam-end fracture, is introduced in the practical design and its validity is verified.

2. EFFECTS OF FRACTURE TOUGHNESS ON BEAM-FLANGE FRACTURE STRENGTH

Tension tests of welded joints with defect were conducted to specify the factors affecting the brittle fracture at beam-ends [2]. As shown in Fig. 1, the test specimens were prepared by forming beam-to-column connections composed of a square tube column and an H-shape beam with through-diaphragm; artificial defects of different sizes were created in the end of welded joints. The test specimens were manufactured in three combinations using different steel plates and welding wire, and the test was conducted using loading velocity and test temperature as parameters. Brittle fractures occured in the vicinity of the defect with ductile cracks in each specimen. Fig. 2 shows the test results. The maximum strength (P_{max}) obtained in the test was normalized by the product of the flange sectional area (A_f) and the tensile strength (σ_u) of steel or weld metal, which was calculated taking into account the change in strength induced by the strain velocity and temperature. P_{max} was compared to the Charpy absorbed energy (${}_vE_{br}$) at the test temperature where brittle fracture occured. ${}_vE_{br}$ was found from the respective energy transition curves of the base metal, the heat-affected zone and the weld metal. These curves had previously been obtained by conducting impact tests on test specimens extracted from welded joints manufactured using the same steel plates, welding wires and welding conditions as those of

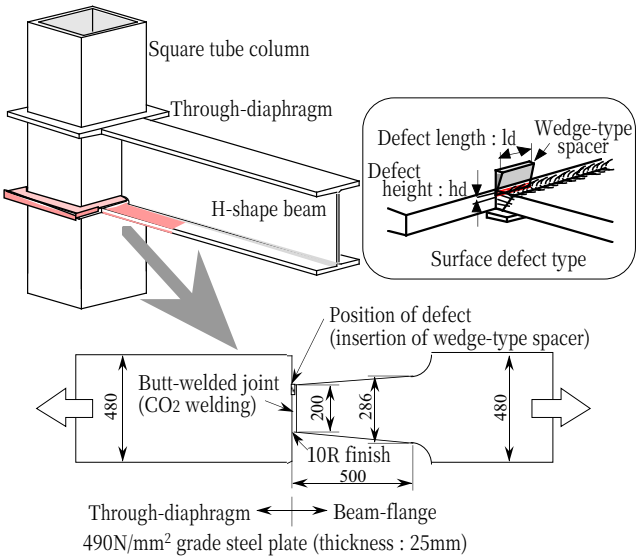

Fig. 1 Tension Tests of Welded Joints with Defect

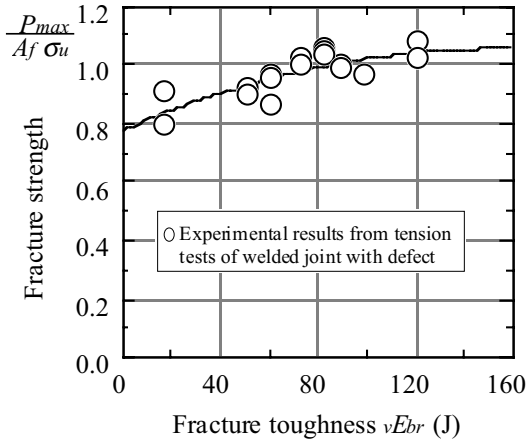

Fig. 2 Relationship between Fracture Toughness and Fracture Strength of Welded Joints

the tension tests. From Fig.2, it was confirmed that there is a positive correlation between ${}_vE_{br}$ and $P_{max}/(A_f \cdot \sigma_u)$.

Cyclic bending tests were also conducted on the T-shaped beam-column subassemblage shown in Fig. 3 [3, 4]. The test specimens, different in the beam-end weld details (type of weld access hole and type of tack welding procedure for backing bar), were manufactured using steel plates and rolled H-shapes having different base metal toughness, and investigations are underway on the ef-

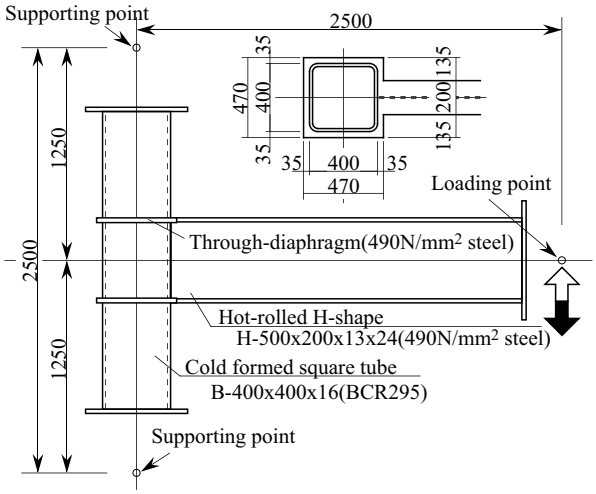

Fig. 3 Cyclic Bending Tests for T-shaped Beam-Column Subassemblages

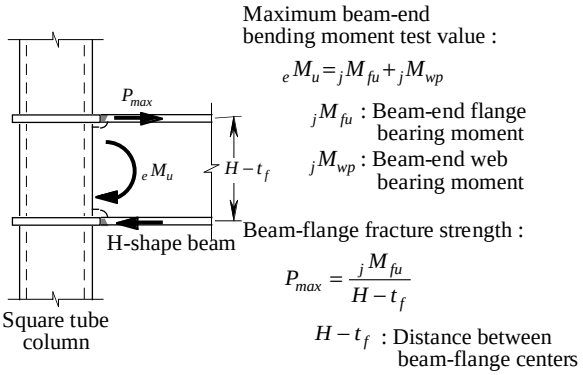

Fig. 4 Estimation of Beam-flange Fracture Strength in the Cyclic Bending Tests

fect of the fracture toughness and weld detail on the fracture strength of the beam-end flange. The beam-end flanges of each test specimen fractured in a brittle manner, and the starting point of fracture was the end of beam-flange welded joint or the toe of the weld access hole. The relationship between maximum tension strength (P_{max}) of beam-flange and fracture toughness ($_vE_{br}$) was investigated as in the following.

P_{max} is found from the maximum beam-end bending moment ($_eM_u$) obtained by the tests, using the method shown in Fig. 4. In the figure, symbol $_jM_{fu}$ indicates the bearing moment of beam flange, H the beam height, t_f the beam flange thickness and $_jM_{wp}$ the assumed value for beam-end web bearing moment calculated based on the literature [5]. $_vE_{br}$ is found from the Charpy impact test on the welded joints manufactured separately, as in the tension tests.

The relationship between $_vE_{br}$ and $P_{max}/(A_f \cdot \sigma_u)$ thus found is shown in Figs. 5 and 6. These figures include the data obtained from the tension test and the existing test results in which $_vE_{br}$ was already been confirmed [6]. Fig. 5 shows the relationship from the test results of specimens in which fracture occurred at the end of beam-flange welded joint, and Fig. 6 those in which fracture occurred from the toe of the weld access hole. Both figures

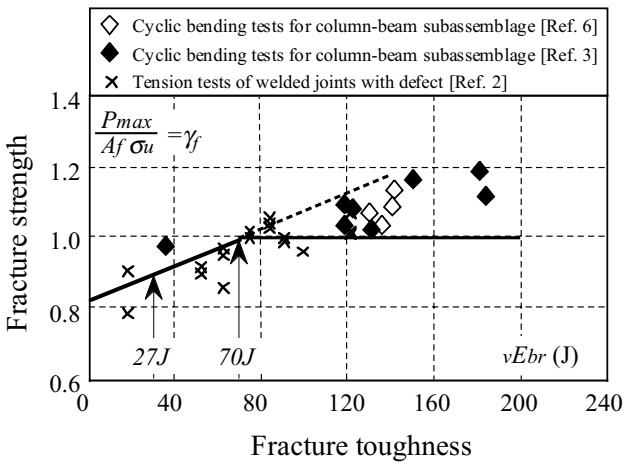

Fig. 5 Relationship between Fracture Toughness and Fracture Strength of Welded Joints (Fracture Initiating from the Beam-flange Weld)

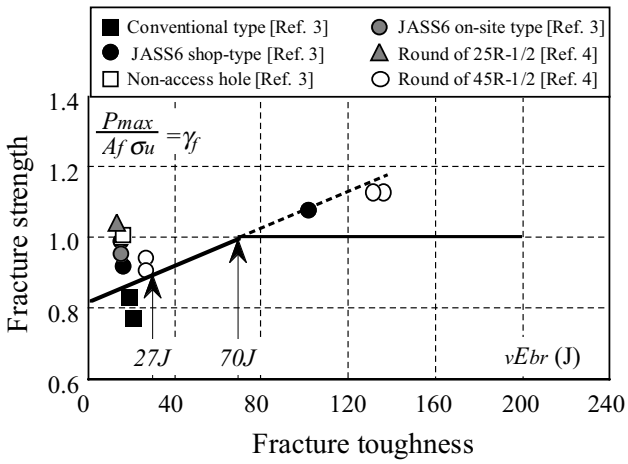

Fig. 6 Relationship between Fracture Toughness and Fracture Strength of Welded Joints (Fracture Initiating from the Toe of the Weld Access Hole)

show that as ${}_{v}E_{br}$ becomes large, $P_{max}/(A_f \cdot \sigma_u)$ tends to become large. Further, it has been found from Fig. 6 that the fracture strength significantly lowers in the conventional type which was the combination of the weld access hole to cause high stress concentration and the tack welding to lower the fracture toughness of base metal.

From these test results, it is considered that the fracture strength of the beam-flange welded joints is decided by the fracture toughness with the adoption of improved-type weld access hole for reducing stress concentration and the restiriction for tack welding on the toe of weld access hole. After all, structural designers can set the beam-flange fracture strength by adopting the appropriate weld details and further by adopting appropriate steels, welding wires and welding conditions so as to secure the fracture toughness of welded joints.

3. ASSESMENT FOR DEFORMATION CAPACITY OF BEAMS

As shown in Fig. 7, when the bending moment of triangle distribution occurs at the beam due to the action of shear force during earthquake, the expansion of beam-end plastic region is decided by the ratio ($\alpha = {}_{j}M_u / {}_{b}M_p$) of the maximum beam-end bending strength (${}_{j}M_u$) to the beam's full plastic moment (${}_{b}M_p$). As α becomes larger, that is, as ${}_{j}M_u$ becomes larger, the plastic region expands and the deformation capacity of beams becomes larger. ${}_{j}M_u$ is expressed as

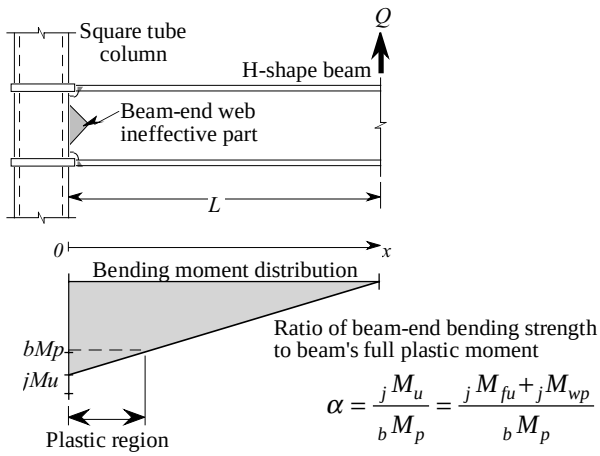

Fig. 7 Assessment Method for Deformation Capacity of Beam-end

$$ {}_{j}M_u = {}_{j}M_{fu} + {}_{j}M_{wp} \tag{1} $$

where ${}_{j}M_{fu}$ and ${}_{j}M_{wp}$ are the maximum bending moment which the beam-flange and the beam-web can bear respectively.

${}_{j}M_{fu}$ is calculated from the plastic section modulus of beam-flange (${}_{f}Z_p$), the tensile strength of beam (σ_u), and the welded joint fracture strength coefficient (γ_f), where γ_f is defined as the normalized fracture strength $P_{max}/(A_f \cdot \sigma_u)$ in this paper.

$$ {}_{j}M_{fu} = {}_{f}Z_p \cdot \sigma_u \cdot \gamma_f \tag{2} $$

On the other hand, ${}_{j}M_{wp}$ is affected by the shape and dimension of columns to which beams are attached. It is known that, in the case of square tube columns, the out-of-plane deformation is generated on the column skin plate section to which the beam-web is attached and the beam-web's bending moment to be transferred to the column becomes small. In the literature [5], the expression to calculate the effective height (χ) and ${}_{j}M_{wp}$ at the beam-end is shown. Here, when using β, the ratio of ${}_{j}M_{wp}$ to the full plastic moment of beam web, ${}_{j}M_{wp}$ is expressed as

$$ {}_{j}M_{wp} = {}_{w}Z_p \cdot \sigma_y \cdot \beta \tag{3} $$

where ${}_{w}Z_p$ is the plastic section modulus of beam-web, and σ_y the yield point of beam.

${}_{b}M_p$ is expressed as

$$ {}_{b}M_p = Z_p \cdot \sigma_y = \left({}_{f}Z_p + {}_{w}Z_p \right) \cdot \sigma_y \tag{4} $$

and therfore, the following expression to calculate α is obtained from Eqs. (1) to (4), using the yield ratio ($YR = \sigma_y / \sigma_u$) .

$$ \alpha = \frac{{}_{j}M_u}{{}_{b}M_p} = \frac{\gamma_f}{YR} \cdot \frac{{}_{f}Z_p}{Z_p} + \beta \cdot \left(1 - \frac{{}_{f}Z_p}{Z_p} \right) \tag{5} $$

According to Navier's assumption, the relation between the moment (M) and the curvature (ϕ) at any section of beam can be found from the stress-strain relation of the steel. Further, the deflection of beams can be calculated by integrating two times along the axis of beam the curvature (ϕ) at respective sections, which conforms to the acting moment (M). As shown in Fig. 7, in the case when

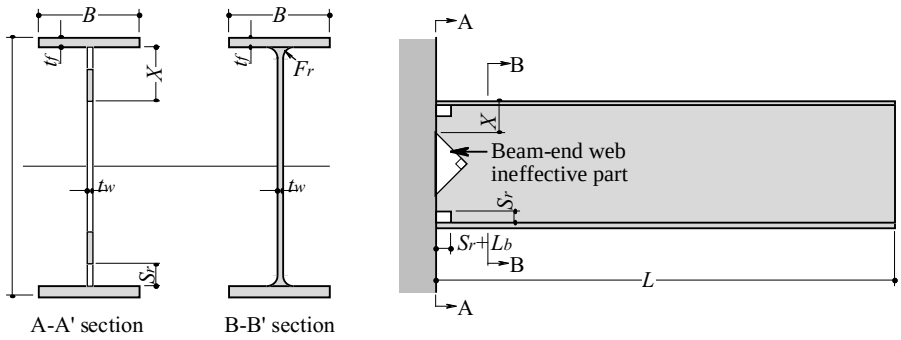

Fig. 8 Cantilever Beam Model Taking into Account the Effective Height of Beam-end Web

the shear force (Q) acts on the cantilever beam-tip without axial force, the beam-end bending moment (${}_bM$) and the beam's relative rotation (${}_b\theta$) can be found from

$$ {}_bM = Q \cdot L \tag{6}$$

$$\theta_b = \frac{\delta}{L} = \int_0^L \int_0^x \phi \cdot dx \cdot dx = \int_0^L \frac{L-x}{L} \cdot \phi \cdot dx \tag{7}$$

$$\phi = F^{-1}(M) \tag{8}$$

where L indicates the cantilever beam length, and $F(\ )$ the function for the $M-\phi$ relation.

Using the above numerical integral (7), the beam's relative rotation decided by the beam-flange fracture is calculated at the time when the beam-end reaches the maximum bending strength. Meanwhile, it has been confirmed by comparing to the test value that the Q-${}_b\theta$ relation of the beam attached to the square tube column can be found by use of the beam model for which the sectional defect, as shown in Fig. 8, is assumed to exist on the beam-end web [2].

4. EXPRESSION TO CALCULATE DEFORMATION CAPACITY LIMITED BY FRACTURE

In the following, a simple expression that can calculate the beam's relative rotation without numerical integral in expression (7) is introduced.

4.1 Basic Expression to Calculate Deformation Capacity of Beams

In this paper, the modified Menegotto-Pinto model proposed in the literature [7], as shown in Fig. 9, is used as the stress-strain (σ-ε) relation of beam.

In the figure, symbol E is the Young's modulus, and R and γ the material constant. Various kinds of models were set for 5 kinds of YR=60, 65, 70, 75 and 80% for 400 N/mm^2 grade steels and 4 kinds of YR=65, 70, 75 and 80% for 490 N/mm^2 grade steels. Material constants of each model is shown in Table1.

Concerning the beam sections, the sections shown in Fig.10 were chosen from among those widely used in the current structural designs, and the M-

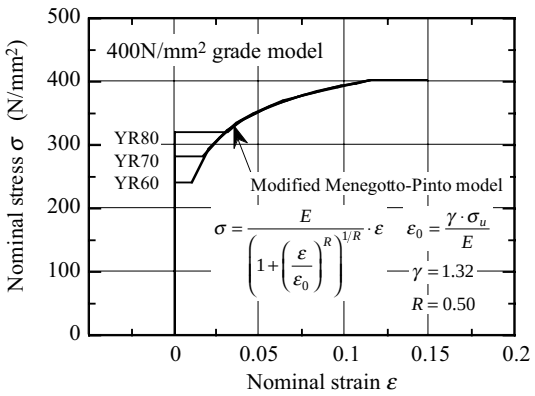

Fig. 9 Stress-Strain Curve Models

Table 1 Assumed Mechanical Properties of Beams

Grade	Yield ratio YR (%)	Yield point σ_y (N/mm^2)	Tensile strength σ_u (N/mm^2)	Uniform Elongation ε_u (%)	Material constant γ	Material constant R
400 N/mm^2	60	240	400	15	1.32	0.50
	65	260				
	70	280				
	75	300				
	80	320				
490 N/mm^2	65	319	490	15	1.26	0.56
	70	343				
	75	368				
	80	392				

ϕ relation of beams was calculated for that sections using the σ-ε relation. The results, which were normalized by the yielding curvature ($\phi_y = 2\varepsilon_y / H = 2\sigma_y / (H \cdot E)$) and ${}_bM_p$, are shown in Fig. 10. Because the M-ϕ relation is nearly same regardless of the beam section, the part of the rise in yield strength due to strain hardening (A-B point in Fig. 11) is approximated using the Ramberg-Osgood function

$$\frac{\phi}{\phi_y} = \frac{M}{{}_bM_p} + a \cdot \left(\frac{M}{{}_bM_p} \right)^b \tag{9}$$

where a and b are the coefficient settled by the yield ratio YR, and as a result of approximation became the value shown in Table 2.

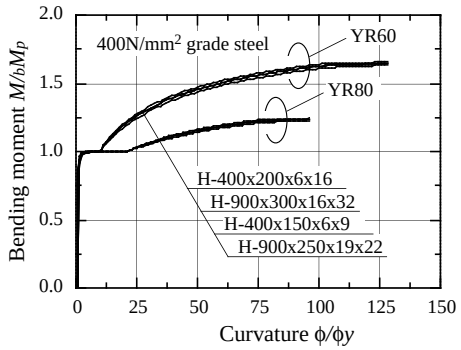

Fig. 10 Bending Moment-Curvature Relation of Beams

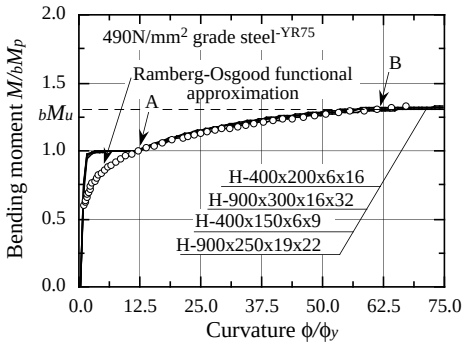

Fig. 11 Mathematical Expression of Bending Moment-Curvature Relation

Table 2 Coefficient of Ramberg-Osgood Function

【400N/mm^2 grade steel】			【490N/mm^2 grade steel】		
YR	*a*	*b*	*YR*	*a*	*b*
0.60	8.25	5.22	—	—	—
0.65	11.2	5.34	0.65	7.41	5.47
0.70	13.4	5.63	0.70	9.31	5.74
0.75	16.0	6.21	0.75	11.2	6.21
0.80	20.1	6.73	0.80	13.8	6.78

The relative plastic rotation θ_{bp} excluding the elastic deformation from ${}_b\theta$ obtained by Eq. (7), is found from

$$\theta_{bp} = \phi_y \cdot \int_0^L \frac{L-x}{L} \cdot \frac{\phi_p}{\phi_y} \cdot dx \tag{10}$$

where ϕ_p is the plastic element of ϕ.

As shown in Fig. 12, the vertical axis (M-axis) of the M-ϕ relation (in Fig. 11) is squared with the axis of cantilever beam (x-axis in Fig. 12). From the figure, the curvature's plastic element (ϕ_p / ϕ_y) and the plastic region (L_p) are expressed as

$$\frac{\phi_p}{\phi_y} = a \cdot \left(\frac{L-x}{L} \cdot \alpha_1 \right)^b \tag{11}$$

$$L_p = L - \frac{L}{\alpha_1} \tag{12}$$

where $\alpha_1 = {}_bM_u / {}_bM_p$, ${}_bM_u$ is the beam's own maximum bending strength.

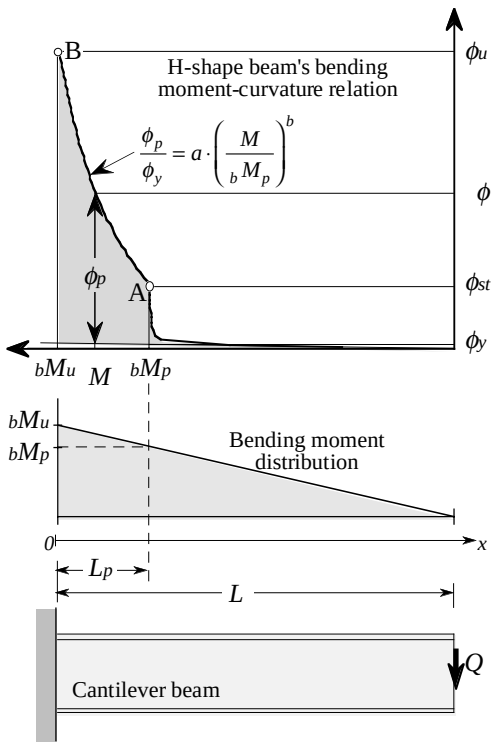

Fig. 12 Cantilever Beam Subjected to Shear Force

When setting the integral range in Eq. (10) up to the range from ${}_bM_p$ to ${}_bM_u$ and substituting Eqs. (12) and (15) for Eq. (10), the expression to calculate the beam's maximum relative plastic rotation (${}_a\theta_{bpm1}$) at the time when the beam-end reaches ${}_bM_u$ is obtained.

$$ {}_a\theta_{bpm1} = \frac{2}{H}\cdot\frac{\sigma_y}{E} \times\int_0^{L_p} \frac{L-x}{L}\cdot a\cdot\left(\frac{L-x}{L}\cdot\alpha_1\right)^b\cdot dx \quad (13) $$

This expression is to indicate the geometrical moment of area around the $M=0$ axis in the section colored pertaining to the M-ϕ relation in Fig.12.

4.2 Expression for Deformation Capacity Limited by Brittle Fracture

Examinations were made on the case in which the brittle fracture occurs at the beam-end before the beam-end reaches the beam's own maximum bending strength (${}_bM_u$). When the full section of the beam web at the beam-end is effective, the ultimate bending moment of beam-end (${}_jM_{u0}$) is expressed by

$$ {}_jM_{u0} = \gamma_f\cdot\sigma_u\cdot{}_fZ_p + \sigma_y\cdot{}_wZ_p \quad (14) $$

In this case, the maximum relative plastic rotation limited by fracture (${}_a\theta_{bpm0}$) can be calculated by replacing ${}_bM_u$ in Fig. 12 with ${}_jM_{u0}$.

$$ {}_a\theta_{bpm0} = \frac{2}{H}\cdot\frac{\sigma_y}{E} \times\int_0^{L_{p0}} \frac{L-x}{L}\cdot a\cdot\left(\frac{L-x}{L}\cdot\alpha_0\right)^b\cdot dx \quad (15) $$

$$ L_{p0} = L - \frac{L}{\alpha_0} \quad (16) $$

$$ \alpha_0 = \frac{{}_jM_{u0}}{{}_bM_p} = \frac{\gamma_f}{YR}\cdot\frac{{}_fZ_p}{Z_p} + \left(1-\frac{{}_fZ_p}{Z_p}\right) \quad (17) $$

4.3 Expression Taking into Account the Lowering of Bending Strength at Beam-end Web

In the case of joining the H-shape beam with the square tube column, the M-ϕ relation in the vicinity of column surface becomes different from the M-ϕ relation in Fig.11. Here, as shown in Fig. 13, it is assumed that as the target sectional area separates from the column, the web section that does not contribute to the bending strength decreases. The figure shows that the M-ϕ relation has changed at the general beam section ($a-a'$ section in the figure) and the beam-end section ($c-c'$), and further at their intermediate section ($b-b'$). In order to calculate the beam's maximum plastic rotation (${}_a\theta_{bpm}$) using the method mentioned above, it is necessary to find the curve that connects the intersection of the x coordinate and the M-ϕ relation at each section (ex. points A, B and C in the figure). Here, if the beam-web bending strength decreases linearly between the points A and C in the figure, ϕ_p is to be expressed as

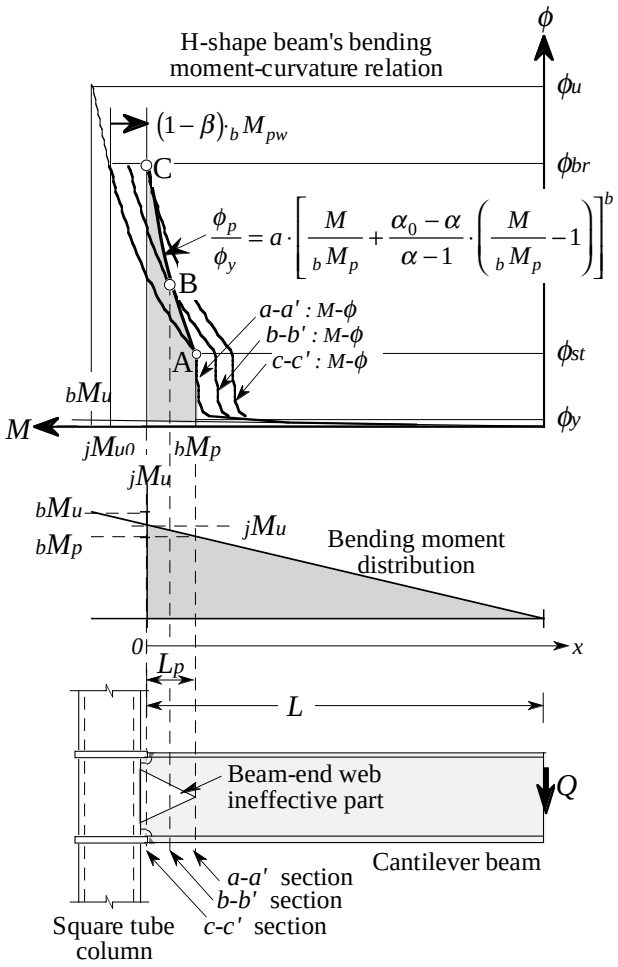

Fig. 13 Cantilever H-shape Beam Joined with Square Tube Column Subjected to Shear Force

$$\frac{\phi_p}{\phi_y} = a \cdot \left[\frac{M}{{}_b M_p} + \frac{\alpha_0 - \alpha}{\alpha - 1} \cdot \left(\frac{M}{{}_b M_p} - 1 \right) \right]^b \qquad (18)$$

where, using α defined by Eq. (5), L_p is given by

$$L_p = L - \frac{L}{\alpha} \qquad (19)$$

With these, the maximum relative plastic rotation of H-shape beam connected to square tube column (${}_a\theta_{bpm}$) can be calculated using the following expression.

$$\begin{aligned} {}_a\theta_{bpm} &= \frac{2}{H} \cdot \frac{\sigma_y}{E} \cdot \int_0^{L_p} \frac{L-x}{L} \cdot a \\ &\times \left[\frac{L-x}{L} \cdot \alpha \cdot \left(1 + \frac{\alpha_0 - \alpha}{\alpha - 1} \right) - \frac{\alpha_0 - \alpha}{\alpha - 1} \right]^b \cdot dx \\ &= \frac{\sigma_y}{E} \cdot \frac{2L}{H} \cdot \frac{a \cdot (\alpha - 1)}{(b+1) \cdot (b+2) \cdot (\alpha_0 - 1)^2 \cdot \alpha^2} \\ &\times \left\{ {\alpha_0}^{b+1} \cdot \left[(b+1) \cdot (\alpha_0 - 1) \cdot \alpha + (\alpha_0 - \alpha) \right] \right. \\ &\left. - \left[(b+1) \cdot (\alpha_0 - 1) + (\alpha_0 - \alpha) \right] \right\} \end{aligned} \qquad (20)$$

5. EFFECTS OF DESIGN FACTORS ON THE DEFORMATION CAPACITY OF BEAM

The numerical calculation was made to investigate the effect of YR and γ_f on the deformation capacity of beam limited by beam-end fracture, which is defined by the maximum relative plastic rotation (${}_a\theta_{bpm}$) in this paper. In parallel with this, verification was made of the simple expression to calculate ${}_a\theta_{bpm}$. For the stress-strain relation of steels, the model in Fig. 9 was used. For each combination of square tube columns and H-shape beams shown in the Table 3, $\alpha = {}_j M_u / {}_b M_p$ and ${}_a\theta_{bpm}$ were computed by Eqs. (5) and (7) respectively. The plots in the Figs. 14 to 16 show the calculation results obtained by numaerical integral. It was found from any figure that the increase of ${}_a\theta_{bpm}$ accompanied by the rise in α is clearly indicated and thus α is effective as one of the parameters to evaluate the plastic deformation capacity.

Fig. 14 indicates the effect of the shear span ratio (L/H) at γ_f=1.0. It is clear from the figure that when L/H becomes small, ${}_a\theta_{bpm}$ becomes small. Fig. 15 indicates the effect of YR at γ_f=1.0 and L/H=10. Already, the effect of YR is included in α at the abscissa. As a result, as YR becomes smaller, the calculation results shift to the righter side, and along with this shift ${}_a\theta_{bpm}$ too becomes larger. Further, Fig. 16 indicates the effect of γ_f, in which ${}_a\theta_{bpm}$ significantly lowers at γ_f=0.8. In addition, it is recognized that in the case of high YR it has become nearly impossible to expect the plastic deformation capacity.

In Figs. 14 to 16, the calculation results of ${}_a\theta_{bpm}$ by means of the simple expression (20) proposed in this paper are shown using the solid line. The solid lines and the plotted groups show favorable correspondences, thus verifying the validity of the expression.

6. CONCLUSION

This paper shows that the fracture toughness of welded joints is a main factor to affect the occurrence conditions for beam-end brittle fracture and decides the beam-flange fracture strength with certainly restricting the weld detail. Further, the simple design expression based on the beam-flange

Table 3 Sectional Shape/Dimension and Yield Strength/Tensile Strength of Columns and Beams

Calculation target	Square tube column	H-shape beam
BCR295+SN400	Roll-formed square tube (a total of 46 kinds) B-200x6 ~ B-550x22 $_c\sigma_y$=295N/mm²	Rolled H-shape (a total of 212 kinds) H-400x150x6x9 ~ H-900x300x19x32 σ_u=400N/mm², σ_y : set using *YR*
BCP325+SN490	Press-formed squre tube (a total of 133 kinds) B-300x9 ~ B-1000x40 $_c\sigma_y$=325N/mm²	Rolled H-shape (a total of 212 kinds) H-400x150x6x9 ~ H-900x300x19x32 σ_u=490N/mm², σ_y : set using *YR*

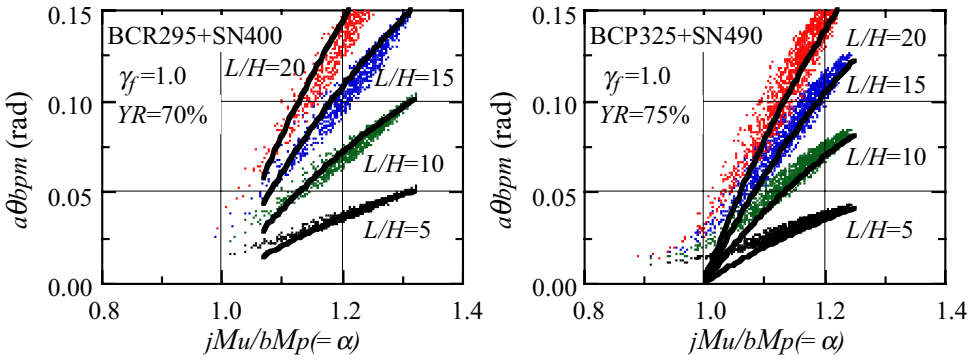

Fig. 14 Effects of Shear Span Ratio on Maximum Plastic Rotation

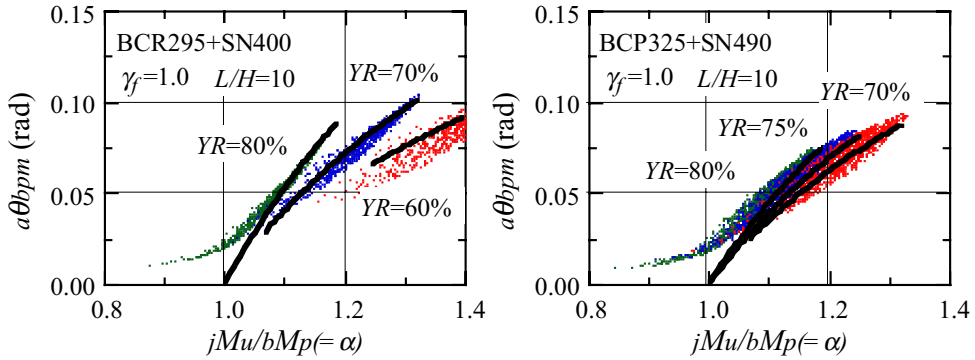

Fig. 15 Effects of Yield Ratio on Maximum Plastic Rotation

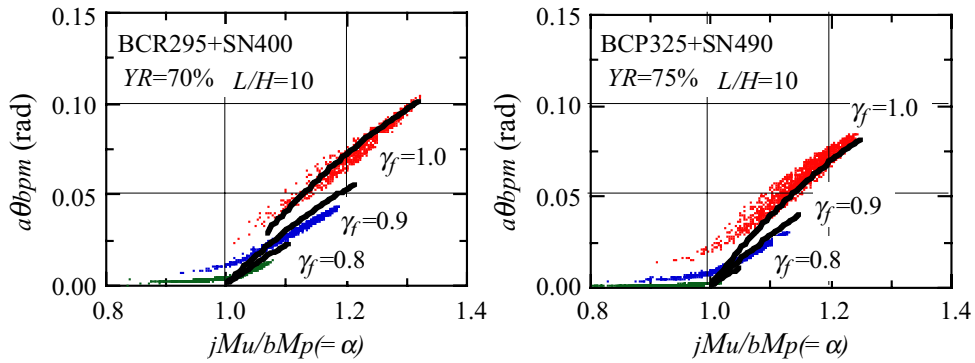

Fig. 16 Effects of Welded Joint Fracture Strength Coefficient on Maximum Plastic Rotation

fracture strength was proposed for calculating the plastic deformation capacity of welded beam-ends limited by brittle fracture. The validity of the expression was also shown.

It has become possible to forecast the rotation demand of beam-end during a severe earthquake using dynamic analysis and so on. Accordingly, it is now possible for structural designers to calculate the rotation of beam-end retained up to the fracture using the approach proposed in this paper and to prevent the brittle fracture that was observed in the Hyogo-ken Nanbu Earthquake by confirming that the retained rotation is larger than the demand.

The use of steels with a low yield ratio for beam is important in order to provide a larger retained rotation than the demand. Further, in order to gain the expected beam-flange fracture strength, it is necessary to select steels and welding wires for

which the fracture toughness of the beam-end welded joint (weld metal, base metal and heat-affected zone) can be secured.

8. REFERENCES

1. Kato, B. and Nakao, M. : Strength and Deformation Capacity of H-shaped Steel Members Governed by Local Buckling, J. Struct. Constr. Eng., AIJ, 1994.
2. Suzuki, T., Ishii, T., Morita, K. and Takanashi, K. : Experimental Study on Fracture Behavior of Welded Beam-to-column Joint with Defects, Steel Construction Engineering, JSSC, 1999.
3. Ishii, T., Kikukawa, S., Morita, K. and Takanashi, K. : Experimental Study on Fracture Behavior of Beam-to-column Connection, Steel Construction Engineering, JSSC, 1999.
4. Azuma, K., Suzuki, T. and Morita, K. : Experimental Study on Fracture Behavior of Built-up H-shaped Beams Connected with Rectangular Hollow Section Columns, Steel Construction Engineering, JSSC, 2000.
5. AIJ : Recommendation for Limit State Design of Steel Structures, 1998.
6. Harada, Y., Morita, K., Yamaguchi, D. and Ishii, T. : Experimental Study on Brittle Fracture in Beam-to-column Connections, Steel Construction Engineering, J. Struct. Constr. Eng., AIJ, 1999.
7. Aoki, H., Kato, B. and Ding, F. : Mechanical Properties of Thick Steel Plates by Blast Furnace and Mathematical Expression for the Stress-strain Diagrams, J. Struct. Constr. Eng., AIJ, 1989.

ACKNOWLEDGEMENTS

The authors' research has been conducted under General Technology Development Project of the Ministry of Construction (currently Ministry of Land, Infrastructure and Transport) entitled Development of Structural Safety Improvement Technology Utilizing New Generation Steel. The authors wish to express their sincere gratitude to all researchers involved in the Project.